Modeling and Simulation of an Electrified Drop-Tube Calciner

Martin H. Usterud Ron M. Jacob Lars-André Tokheim

Department of Process, Energy and Environmental Technology, University of South-Eastern Norway
{137010, Ron.Jacob, Lars.A.Tokheim}@usn.no

Abstract

About 65 % of the carbon dioxide emissions from a modern cement kiln system are generated through calcination (decarbonation). The calcium carbonate in the limestone is the primary source of CO_2, and the rest comes from fuel combustion. This gives a calciner exit gas consisting of N_2, O_2, CO_2, and H_2O, the CO_2 constituting up to 30 % of the mixture. In the future, electric power will have to come from renewable energy. Electrification of the calciner, i.e., replacing fuel combustion with electrically generated heat, will eliminate the fuel combustion exhaust gases. The calciner exit gas will then be pure CO_2 and removes the need for a separate CO_2 capture plant. Such a process may require a new type of calcination reactor, different from the currently used reactors in most cement kiln systems. In the current work, an electrically heated drop-tube reactor (DTR) is used to calcine the meal. The DTR may replace the traditional entrainment calciner. Essential characteristics in developing a DTR include the particle size distribution (PSD), particle settling velocity, operational temperature of the tube wall, and velocity of the product gas. A PSD ranging from 0.2 to 180 µm, where most particles have a diameter < 30 µm, was investigated. Also, to assess the effect of clustering, an effective particle diameter of 500 µm was evaluated. Two different DTR designs were compared, 1) co-current flow of gas and particles, 2) counter-current flow of gas and particles. The dimensions of a calcination reactor were calculated using simulations in Python 3.8. The tube diameter was selected as the key parameter to see how the overall design of the reactor was influenced.

Keywords: Drop tube reactor, electrification, CO_2 capture, calcination, Python 3.8

1 Introduction

Concrete is one of the most used construction materials in the world. The key additive in concrete is cement, and about 4.1 billion tonnes of cement are produced globally every year, resulting in a global anthropogenic CO_2 emission of up to 8 % (Andrew, 2018). Hence, strategies such as improving the energy efficiency of existing cement plants and using lower carbon fuels and green electricity to decarbonize the raw meal should be implemented (Norcem, 2021).

Producing cement clinkers has two significant sources of CO_2 emission: calcination of the raw materials and fuel combustion. Calcination is a thermally driven chemical reaction where the calcium carbonate ($CaCO_3$) in the limestone will decompose and form lime (CaO) and CO_2: $CaCO_3 + heat \rightarrow CaO + CO_2$. The decarbonation of raw meal accounts for about 65 % of the CO_2 emissions in a modern cement kiln system, while fuel combustion accounts for about 35 % (Tokheim et al., 2019).

Modern calciners are based on raw meal particles being entrained by hot combustion gases, which at the same time provide the required heat transfer to the particles. However, expecting a greener future, the cement clinker production process will have to be powered by electricity generated by renewable energy sources. Implementing green electricity to power the calciner instead of fossil fuels can prove to be an efficient way to reduce CO_2 emissions: The CO_2 produced from the standard fuel combustion is eliminated, and the CO_2 produced from the calcination process is pure, which removes the need for a separate CO_2 capture facility.

Different reactors may be applied in a process where the heat is transferred indirectly to the meal, for example rotary calciners (Tokheim et al., 2019), fluidized bed calciners (Samani et al., 2020), or drop tube calciners.

Calcination by indirect heat transfer in drop tube calciners has been tested in the Leilac project (Leilac, 2021), but in that project, fuel combustion is the source of energy used for calcination (Hills et al., 2017; Hodgson et al., 2018).

In this work, we study indirect heat transfer in an electrified drop tube reactor and address the following key questions:

- What is the settling velocity of the particles?
- How will the CO_2 from the calcination reaction impact the particle flow in the reactor?
- What factors are decisive for the tube diameter and length?

The purpose of this study is to investigate, through modeling and simulation, how variable design parameters and operational settings will impact the industrial calcination in an electrified DTR. Two different designs are considered; co-flow and counter-flow of meal and gas.

2 Method

To design an electrically heated DTR in order to calcine the raw meal, the particle settling process and the heat transfer from the heated tube wall to the particles in the reactor are modelled. A modified shrinking core model (SCM) is used to study the kinetics of the calcination reaction. The reaction rate coefficient of the reaction, which is dependent on the equilibrium pressure and the partial pressure of CO_2, is modelled. The models are implemented in Python 3.8 for simulation purposes to investigate how different particle sizes, wall temperatures, and fluid velocities will impact the system design.

3 Process description

The upper part of Figure 1 shows a typical modern cement kiln system. The raw meal is preheated in two preheaters before being calcined in the calciner. The precalcined meal is then sent to a rotary kiln, where the meal is fully calcined and cement clinker is produced. Finally, the clinker is cooled in a clinker cooler.

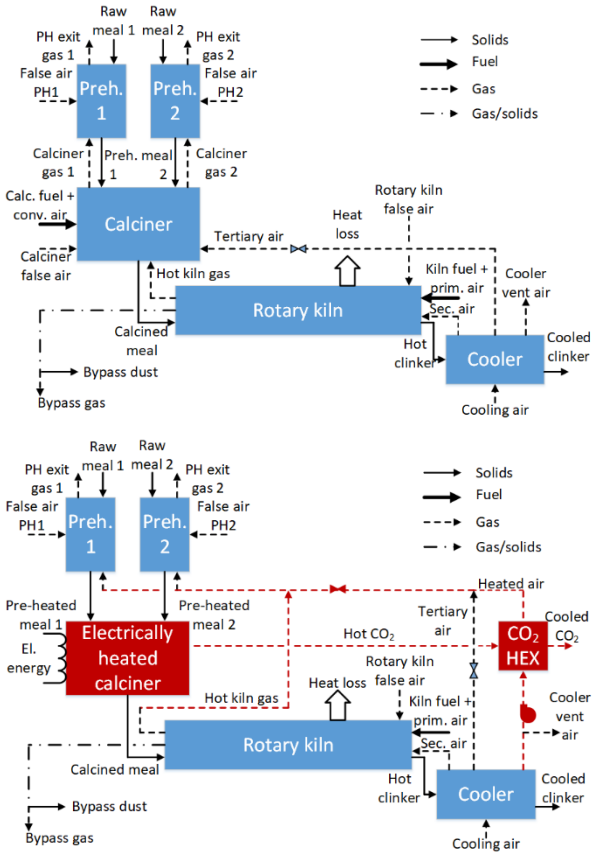

Figure 1. A regular cement kiln system with two preheater strings (top) and a system equipped with an electrified calciner (bottom) (Tokheim et al., 2019).

The lower part of Figure 1 shows a system where the fuel-fired calciner has been replaced by an electrified calciner. The fuel in the calciner fuel has now been replaced by heat provided from electrical energy. The combustion air is no longer required, so this air stream and the hot rotary kiln exit gas are both routed to the preheater, where the sensible heat can be utilized. Hence, the only gas component in the exit gas stream from the calciner is CO_2 coming from the decarbonation. The red-colored process units in Figure 1 are considered in the present study.

Figure 2 shows a process flow diagram of a DTR (i.e., the electrically heated calciner) and adjacent units such as a de-dusting cyclone, a heat exchanger, and a fan.

The preheated raw meal enters the top of the reactor at a temperature of about 650 °C. As the particles continuously fall through the reactor, the heat generated from electricity will heat the particles to a calcination temperature of about 900 °C. During the calcination of the particles, CO_2 is produced. A fan is implemented to force the normally buoyant gas down through the bottom of the DTR, as shown in Figure 2. A de-dusting cyclone is implemented to separate the particles and exit gas. Heat exchangers cool down the pure CO_2 gas before it is sent to storage or further processing. The calcined meal is sent to the rotary kiln. In this study, two different DTR designs are compared; co-current flow of gas and particles (shown in Figure 2), and counter-current flow of gas and particles. In the latter concept, the CO_2 will exit at the top of the DTR instead of at the bottom, but otherwise the flow diagram will be the same.

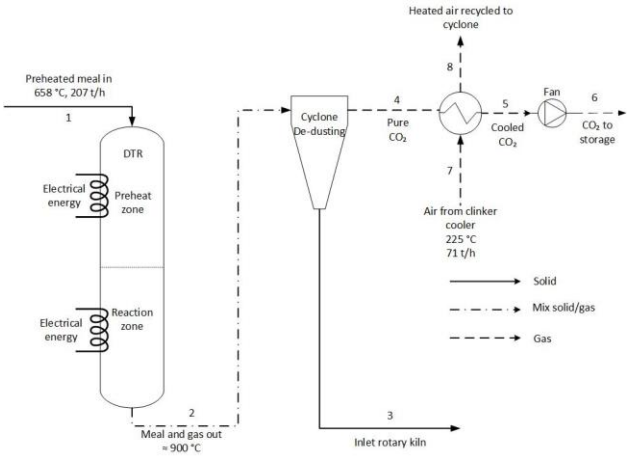

Figure 2. Process flow diagram of DTR and adjacent units.

Implementing the DTR in an existing cement kiln system is expected to have a relatively small constructional impact: 1) Replacement of the existing entrainment calciner with the DTR, 2) Installation of de-dusting cyclone(s), 3) installation of heat exchanger(s) for utilization of sensible heat in the hot CO_2 and 4) installation of a fan to pull the CO_2 out of the calciner and send it to a CO_2 processing unit (required for storage and transport).

The DTR itself will have to be implemented in the form of a number of parallel tubes, each processing a fraction of the preheated meal.

Figure 3 shows the cumulative particle size distribution of a typical raw meal, collected from

Norcem AS Brevik. The diameter ranges from 0.2 to 180 µm.

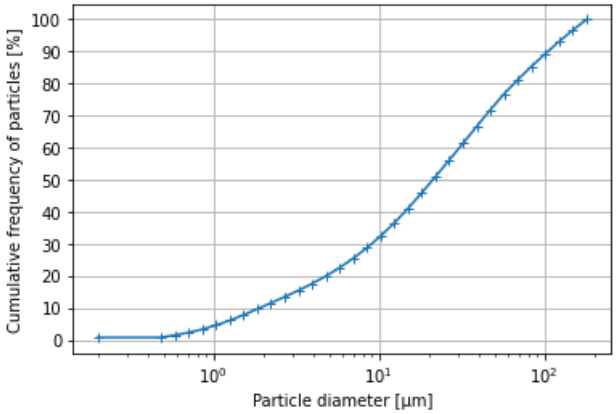

Figure 3. Cumulative frequency of particles with a size range of 0.2-180µm in diameter.

Table 1. Design basis values.

Parameter	Unit	Value
Feed rate of raw meal	t/h	207
Fraction of calcium carbonate in raw meal	kg/kg	0.776
Calcination degree	%	94
Reference temperature	K	298
The temperature of the preheated meal	K	931
Calcination temperature	K	1173
Wall temperature	K	1323
Overall heat transfer coefficient	W/(m²K)	250
Enthalpy of calcination	MJ/kgCO_2	-3.6
Enthalpy of other meal-related reactions	MJ/kgCO_2	0.3
Electricity-to-heat efficiency	%	98
Emissivity	-	0.9
Gravitational acceleration	m/s²	9.807
Particle diameter	µm	0.2-180, 500
Dynamic viscosity CO_2	Pa s	$4.65 \cdot 10^{-5}$
Density $CaCO_3$	kg/m³	2711
Density CaO	kg/m³	1520
Gas velocity	m/s	0.1-2.0, 0.5
Partial pressure of CO_2	atm	1
Specific heat capacity $CaCO_3$ at 931 K, constant pressure	J/mol K	134
Specific heat capacity $CaCO_3$ at 1173 K, constant pressure	J/mol K	140

Table 1 is a list of design basis values used in the simulations. The input values are the same as used in a previous study, in which a rotary calciner was used in an electrified calcination process (Tokheim et al., 2019).

4 Modelling

The DTR must be dimensioned in such a way that efficient calcination of the raw meal occurs. Thus, the settling velocity of particles, reaction kinetics, mass and energy balances, heat transfer, and design dimensions have been modelled.

4.1 Particle settling velocity

The settling velocity of the particles inside the DTR is modelled as a function of particle diameter. The following simplifications have been made:

- Initial particle acceleration period neglected
- No impact from particle-wall interactions
- Direct transition from laminar to turbulent flow regime (neglecting the transition region)
- No interaction between particles

For small particles, the settling is laminar, and the settling velocity can then be calculated using Equation 1, where g [m/s²] is the gravitational constant, D_p [m] is the particle diameter, μ [Pa·s] is the dynamic viscosity and ρ_p and ρ_{gas} are the densities [kg/m³] of the particle and the gas, respectively (Zevenhoven and Kilpinen, 2001):

$$v_t = \frac{g \cdot D_p^2 \cdot (\rho_p - \rho_{gas})}{18 \cdot \mu} \quad (1)$$

Equation 2 is used to confirm that the Reynolds number, Re_D, indicates laminar settling. If $Re_D < \sim 1$, the flow is in the Stokes regime and regarded as laminar.

$$Re_D = \frac{\rho_{gas} \cdot v_t \cdot D_p}{\mu} \quad (2)$$

However, if the Reynolds number from Equation 2 is found to be larger than ~1, this indicates that the settling is turbulent. Then the Archimedes number is calculated according to Equation 3, whereas an empirical Reynolds number is calculated from Equation 4, and, finally, Equation 5 is utilized to determine the settling velocity in the turbulent flow regime:

$$Ar = \frac{\rho_{gas} \cdot (\rho_p - \rho_{gas}) \cdot g \cdot D_p^3}{\mu^2} \quad (3)$$

$$Re = 0.1334 \cdot Ar^{0.7016} \quad (4)$$

$$v_{t,turb} = \frac{Re \cdot \mu}{\rho_{gas} \cdot D_p} \quad (5)$$

As the calcination reaction occurs within the DTR, the particles are gradually decarbonated, a process that changes the density of the particles. Thus, to compensate for the velocity of the calcined ($v_{94\%,calcined}$) and uncalcined ($v_{uncalcined}$) particles, Equation 6 is used as a representative average value.

$$v_{mid} = \frac{v_{uncalcined} + v_{94\%,calcined}}{2} \quad (6)$$

The effective settling velocity for both designs is calculated by Equation 7 (co-current) and Equation 8 (counter-current).

$$v_{eff,t,co} = v_{mid} + u_m \quad (7)$$

$$v_{eff,t,counter} = v_{mid} - u_m \quad (8)$$

Figure 4 shows the calculated effective settling velocity of the particles. The green and the yellow curves represent the counter-current design, whereas the blue and red lines give the effective settling velocity for the co-current design. These calculations are done with a constant gas velocity of 0.5 m/s (cf. Table 1), and for the counter-current case, the effective velocity is negative for particles smaller than 226 µm.

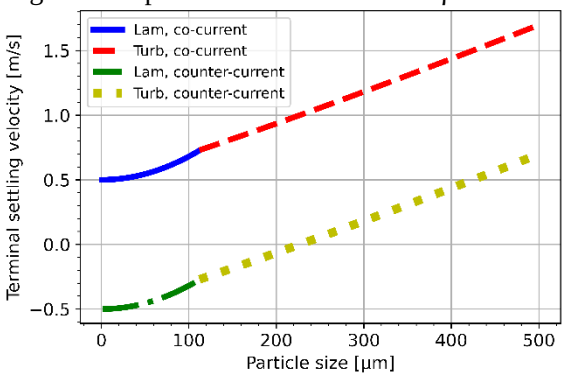

Figure 4. Settling velocity for the counter-current and co-current flow designs as a function of particle diameter. Including laminar and turbulent flow regimes.

In the calculations shown above, it was assumed that the particles do not interact with each other. However, due to the high solids loading in the system, it is likely that the particles will interact with each other and form clusters that effectively behave as bigger particles. This means that the actual settling velocity may be significantly higher than the values calculated above. Hence, in the simulations in Section 5, a larger effective particle diameter was used.

4.2 Reaction kinetics

The shrinking core model (SCM) describes the changes in a particle when a chemical reaction occurs, assuming that the particle size remains unchanged whereas the reaction front will gradually move towards the center of the particle, so that the unreacted core gradually shrinks, from a diameter equal to the particle diameter, to zero.

To calculate the conversion factor of the particles, the correlations and results from (Milne et al., 1990) have been used. The calcination conversion factor is calculated by Equation 9, where k_r [$m^{0.6}$/s] is the reaction rate coefficient, d_0 [$m^{0.6}$] is the initial diameter of the particle and t_{cal} [s] is the calcination time.

$$X = 1 - \left(1 - \frac{k_r}{d_0^{0.6}} \cdot t_{cal}\right)^3 \quad (9)$$

The reaction rate coefficient is determined by implementing the equilibrium pressure, P^* [atm], and partial pressure of CO_2 inside the reactor, P_{CO2} [atm]. These are given by Equations 10 and Equation 11, respectively (Stanmore and Gilot, 2005).

$$k_r = A \cdot \exp\left(\frac{-E}{R \cdot T}\right) \cdot (P^* - P_{CO2}) \quad (10)$$

$$P^* = 4.192 \cdot 10^9 \cdot \exp\left(\frac{-20474}{T}\right) \quad (11)$$

In this study, where CO_2 is the only gas in contact with the meal, and the system is operating at ambient pressure, the partial pressure of CO_2 is assumed to be equal to 1 atm. T [K] is the calcination temperature, which is set to 1173 K in this study. In Equation 10, the pre-exponential factor A is 0.012 mol/(m²·s·kPa), and the activation energy E is 33.47 kJ/mol.

4.3 Mass and energy balance

A mass and energy balance for the DTR at steady-state conditions was conducted, assuming no heat loss to the surroundings.

The mass balance was used to determine the mass flow rate of produced CO_2 from calcination, given by Equation 12, where $\dot{m}_{phm,in}$ [t/h] is the inlet feed rate of preheated meal (cf. Table 1), $\dot{m}_{CO2,prod}$ [t/h] is the mass flow rate of produced CO_2, and $\dot{m}_{meal,cal}$ [t/h] is the mass flow rate of calcined meal.

$$\dot{m}_{phm,in} = \dot{m}_{CO2,prod} + \dot{m}_{meal,cal} \quad (12)$$

Equation 13 is used to calculate the amount of produced CO_2 assuming 100 % conversion from $CaCO_3$ to CaO and CO_2, where $w_{CO2,phm}$ is the weight fraction of CO_2 in the $CaCO_3$. To find the mass flow rate of produced CO_2 at 94 % calcination degree (X), Equation 14 is used (cf. Table 1).

$$\dot{m}_{CO2,phm,100\%} = w_{CO2,phm}\dot{m}_{phm,in} \quad (13)$$

$$\dot{m}_{CO2,prod} = \dot{m}_{CO2,phm,100\%}\, X \quad (14)$$

By dividing the DTR into two section – one preheating and one calcination section – the amount of heat required to process the meal was determined.

Equation 15 is the energy balance for the preheating section, where $E_{el,ph}$ [MW] is the energy supplied into the system to preheat the raw meal to calcination temperature. $C_{p,phm}$ [J/mol K] is the specific heat capacity of the preheated meal (cf. Table 1).

$$E_{el,ph} = \dot{m}_{phm} \cdot C_{p,phm} \cdot (T_{cal} - T_{phm}) \quad (15)$$

Equation 16 is the energy balance for the calcination section based on how much energy must be supplied to the reactor for the reactions to occur. The mass flow rate of CO_2 is calculated based on the mass balance (cf. Equation 13 and 14), and H_{cal} and H_{other} are the enthalpies of reaction for calcination and other meal related reactions, respectively (cf. Table 1).

$$E_{el,cal} = \dot{m}_{CO2,prod} \cdot (H_{cal} + H_{other}) \quad (16)$$

4.4 Radiation heat transfer

The particles are heated by conduction, convection, and radiation heat transfer. However, at the high temperature prevailing in the calciner, radiation heat transfer is much more significant than the two other mechanisms. Thus,

radiation is here assumed to be the only acting heat transfer mechanism.

CO_2 is a polyatomic gas and will absorb some of the radiation, contributing to a reduced effect of the radiation heat flux. The effect of the absorption was investigated and found not to significantly affect the radiation heat flux. Hence, the main effect is the direct radiation from the hot wall to the particles, and this is the mechanism used in the model.

For radiation heat transfer from the hot wall at temperature T_{wall} [K] to the particles at temperature T [K], Equation 17 can be applied to estimate the radiation heat flux, where ε is the wall emissivity and σ is the Stefan-Boltzmann constant ($5.67 \cdot 10^{-8}$ $\frac{W}{m^2 K^4}$) (Incropera et al., 2017).

$$q''_{rad} = \varepsilon \cdot \sigma \cdot (T^4_{wall} - T^4) \quad (17)$$

4.5 DTR design

To effectively process the raw meal to the desired calcination degree, the diameter and heat of the reactor tube have been determined. The diameter of a cylindrical tube is found by Equation 18.

$$D = \sqrt{\frac{4 \cdot A_{cross}}{\pi}} \quad (18)$$

Here, the cross-sectional area, A_{cross} [m²], is given by Equation 19, where $\dot{V}$ [m³/s] is the volumetric flow rate of fluid, and u_m [m/s] is the fluid velocity chosen based on the settling velocity of the particles.

$$A_{cross} = \frac{\dot{V}}{u_m} \quad (19)$$

The necessary heat transfer area of the reactor tube can be determined based on the energy balance and the radiation heat flux calculations, given by Equation 20.

$$A_{heat,preheat} = \frac{Q_{preheat}}{q''_{preheat}} \qquad A_{heat,calcination} = \frac{Q_{calcination}}{q''_{calcination}} \quad (20)$$

Based on the energy required for heating the raw meal to the calcination temperature, the height of the section can be determined with Equation 21.

$$h_{t,preheating} = \frac{A_{heat,preheating}}{\pi \cdot D} \quad (21)$$

The necessary height of the calcination section is found by Equation 22, based on the required residence time of the particles (cf. Figure 5), and the effective particle settling velocity (cf. Figure 4).

$$h_{t,calcination} = t_{res} \cdot v_{eff.t} \quad (22)$$

Further, the total height can be found by Equation 23 by adding the preheating section height ($h_{t,preheating}$) and the calcination section height ($h_{t,calcination}$).

$$h_t = h_{t,preheating} + h_{t,calcination} \quad (23)$$

4.6 Simulations

The models described above were implemented in Python 3.8. Both system designs – co-current and counter-current – are highly dependent on the tube diameter. Thus, the diameter was selected as a key parameter to vary in the determination of the DTR design.

By having a counter-current flow of gas and particles, the buoyant CO_2 gas may be problematic regarding smaller particles. The particles processed in the co-current flow of gas and particles will have an increased effective settling velocity. Thus, the height of the DTR is expected to increase accordingly. However, this design is not impaired by the CO_2 gas, which is forced to flow downwards with the particles.

5 Results and discussion

Figure 5 shows the calcination degree as a function of time and effective particle size. The smaller particles in the PSD have a short calcination time, meaning that complete conversion from $CaCO_3$ to CaO will happen rapidly. Given a calcination time, some of the larger particles may, however, not achieve the desired calcination degree.

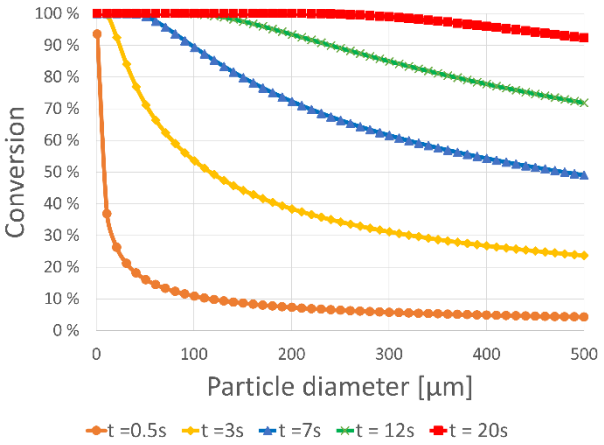

Figure 5. Calcination degree (conversion) as a function of time particle size. The calcination temperature is 1173 K. Each curve represents a given calcination time.

Figure 6 shows the gas velocity and the required number of tubes as a function of the tube diameter. The gas velocity should be low in order to reduce the number of particles being forced out of the reactor by friction (relevant for the counter-current concept).

For the co-current flow of gas and particles, the effective settling velocity increases with increased fluid velocity. Thus, to reduce the height of the tube, the gas velocity should be minimized.

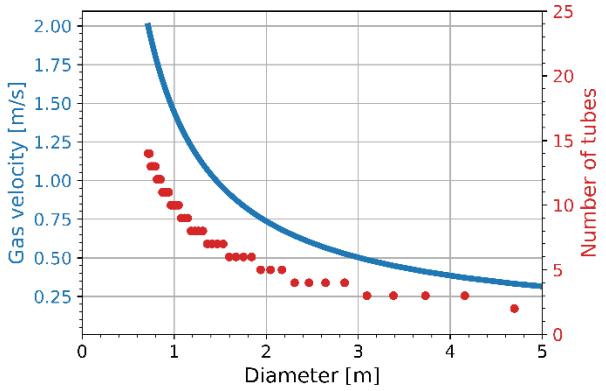

Figure 6. Gas velocity and number of tubes as a function of tube diameter (counter-current flow).

Figure 7 illustrates the reaction process and shows the heat necessary to preheat the raw meal to the calcination temperature, and the calcination reaction assuming 94 % conversion to CaO from $CaCO_3$ in the DTR. A feed rate of 207 t/h generates about 66 t/h CO_2 from the reaction, and about 141 t/h of calcined meal is produced.

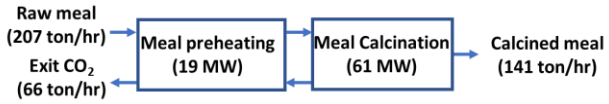

Figure 7. Shows the results from the mass and energy balances listed in Section 4.3.

Figure 8 shows the heat flux with varying temperature. The temperature is varied in the range 1200 – 1500 K, and the green cross marks the flux when operating at 1323 K, which results in a flux of 60 kW/m^2. Increasing the temperature will decrease the required height as then the heat flux increases. However, it may be difficult to find materials that can operate at very high temperatures for a long period of time. A wall temperature of 1323 K (1050 °C) may be a suitable trade-off between heat transfer efficiency and material availability.

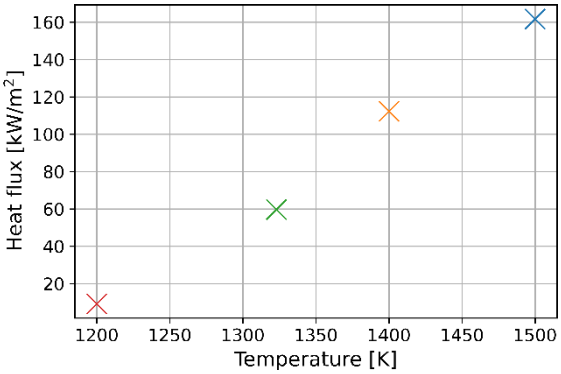

Figure 8. Radiation heat flux as a function of wall temperature.

The upper part of Figure 9 shows the required number of tubes as a function of the diameter. The calculations are based on a constant feed rate of 207 t/h, a residence time of 20 s, a constant gas velocity of 0.5 m/s, effective particle diameter of 500 µm, and wall temperature of 1323 K (cf. Table 1.).

The lower part of the figure shows the tube height (cf. Equation 23), where the slight increase in height comes from the preheating part of the tube, which increases because of fewer processing tubes.

Based on Figure 9, several combinations of diameter, height and number of tubes can be used, depending on the requirements and specifications on the system where it should be installed. However, a relatively small diameter is necessary to ensure efficient heat transfer.

A viable option may be to use 15 processing tubes with a diameter of 2.6 m and a height of 37.6 m, each processing a feed of 13.8 t/h. However, it could be that the heat transfer will be impaired with such a big diameter, and another option could be 40 tubes with a diameter of 1.6 m and a height of 37.5 m, each tube processing 5.3 t/h. If fewer operating DTRs were to be used, the diameter would greatly increase. The efficiency of heat transfer would decrease since the heat may not reach the particles furthest away from the tube wall (the heat source).

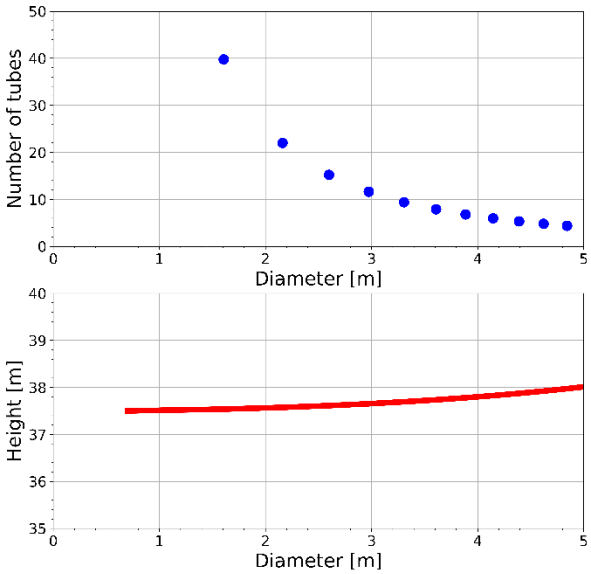

Figure 9. Number of tubes and height necessary to process the raw meal (co-current) as a function of the tube diameter.

Figure 10 shows the number of tubes and the tube height as a function of the tube diameter (counter-current design) for the same conditions as in Figure 9. The most significant difference between Figure 9 and Figure 10 is the tube height due to the effective particle settling velocity (cf. Equations 7 and 8).

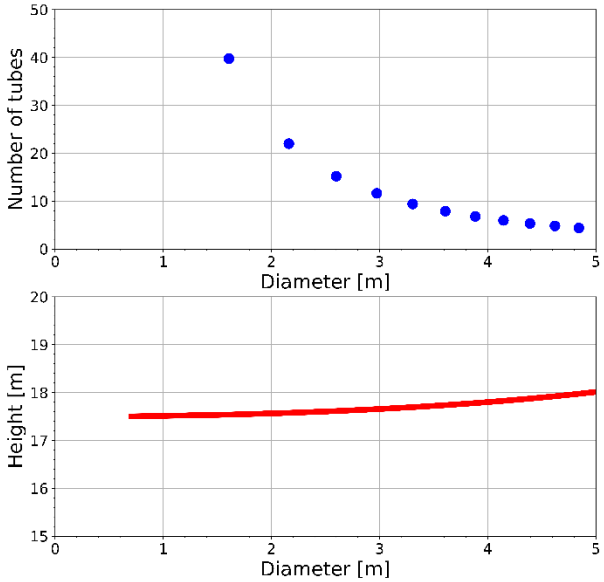

Figure 10. Number of tubes and height necessary to process the raw meal (counter-current) as a function of the tube diameter.

As mentioned before, the difference between the co-current and counter-current design is the impact of the gas velocity on the particles settling velocity. One major consideration when choosing the preferred design is the available area for the installation of the system. If height is a limiting factor at the site where the DTR is to be installed, the counter-current design should be considered.

6 Conclusion

Two concepts were investigated for calcination of raw meal in a drop tube reactor, 1) co-current flow of particles and gas, 2) counter-current flow of particles and gas.

The settling velocity is dependent on the particle size. Small raw meal particles with a low settling velocity will be affected by the buoyant CO_2 gas for the counter-current design if the fluid velocity is 0.5 m/s. This is not the case for the co-current design. However, the required height of the tube increases as a result of the increased settling velocity of the particles.

Due to the high loading of solids in the system, it is likely that the particles will interact with each other and form clusters that effectively behave as bigger particles. The settling velocity is a function of the particle size, and about 1.2 m/s is achieved for particles with an effective size of 500 µm. Using a gas velocity of 0.5 m/s, the effective settling velocity of the particles was accordingly found to be 1.7 m/s and 0.7 m/s for the co-current and counter-current designs, respectively.

Simulations show that operating with a high fluid velocity decreases the diameter of the reactor tube. Larger tube diameters will likely impair the heat transfer.

Both designs are influenced by decreasing the tube diameter. The particles in the co-current design will achieve a higher effective settling velocity, increasing the height of each reactor tube. The particles in the counter-current design will achieve a reduced effective settling velocity, increasing the residence time of the particles and reducing the necessary tube height. However, small particles (with a settling velocity less than the fluid velocity) may be entrained by the buoyant CO_2 gas and exit at the top of the reactor.

Mass and energy balances were used to determine how much heat is required to preheat and calcine the meal, and how much CO_2 is produced during calcination of $CaCO_3$. About 80 MW in total is required for both processes when calcining a feed rate of 207 t/h. The process results in about 66 t/h produced CO_2 and 141 t/h calcined meal.

Increasing the number of processing tubes and dividing the total feed rate of raw meal between the tubes decreases the diameter while ensuring the correct fluid velocity of the gas.

The decisive factor for the tube diameter is the fluid velocity. To achieve an acceptable gas velocity and maintain a high heat transfer coefficient, a relatively high number of processing tubes is required.

Which design (co- or counter-current) and what configuration of the system with regards to diameter, height and number of operating tubes are heavily dependent on the system where the DTR is to be installed. However, if the PSD consist of small particles and the buoyant CO_2 is a problem, then the co-current design should be used. The proposed dimensions by calculations and simulations to ensure efficient heat transfer can be 40 DTRs, each with a diameter of 1.6 m and a height of 37.5 m.

The counter-current flow of gas and particles is impaired if clustering of particles does not occur. For a case with no interaction between the particles, a minimum effective diameter of 226 µm is required to avoid particles rising with the buoyant CO_2 gas when operating with a gas velocity of 0.5 m/s in a counter-current design. If the installation of the DTR system is heavily dependent on minimizing the height of tubes because of height limitations, the counter-current design should be used. Considering the same number of operating DTRs and the same diameter as for the co-current design, the height may then be reduced to 17.5 meters.

In order to numerically verify the results, future work could include CFD simulations of the flow process.

Acknowledgements

This study was carried out as part of the research project "Combined calcination and CO_2 capture in cement clinker production by use of CO_2-neutral electrical energy – Phase 2". Gassnova and Norcem are greatly acknowledged for funding this project.

References

Robbie M. Andrew. Global CO2 emissions from cement production, 1928–2017, Earth Syst. Sci. Data, 10, 2213–2239, https://doi.org/10.5194/essd-11-1675-2019, 2018

Thomas P. Hills, Mark Sceats, Daniel Rennie, and Paul Fennella. LEILAC: Low cost CO_2 capture for the cement and lime industries. Energy Procedia 114, pp. 6166–6170, 2017, doi: 10.1016/j.egypro.2017.03.1753

Phil Hodgson, Mark Sceats, Adam Vincent, Daniel Rennie, Paul Fennell, Thomas Hills. Direct Separation Calcination Technology for Carbon Capture: Demonstrating a Low Cost Solution for the Lime and Cement Industries in the LEILAC Project. 14th International Conference on Greenhouse Gas Control Technologies (GHGT-14), 21st–25th October, Melbourne, Australia, 2018

Frank P. Incropera, David P. Dewitt, Theodore L. Bergman, Adrienne S. Lavine. Principles of heat and mass transfer. John Wiley & Sons, Global edition, 2017.

Leilac, Low Emissions Intensity Lime & Cement, project web site, https://www.project-leilac.eu/, 2021

C. R. Milne, G. D. Silcox, D.W. Pershing, D.A. Kirchgessner. Calcination and sintering models for application to high-temperature, short-time sulfation of calcium-based sorbents. *American Chemical Society*, 29, 139-149, 1990. doi: https://doi.org/10.1021/ie00098a001

Norcem Heidelbergcement Group. *Cement production and emissions*. Retrieved (08.01.2021). Available online: https://www.norcem.no/en/Cement_and_CCS

Nastaran A. Samani, Chameera K. Jayarathna and Lars-André Tokheim. Fluidized bed calcination of cement raw meal: Laboratory experiments and CPFD simulations, Linköping Electronic Conference Proceedings (Proceedings of the 61st SIMS, September 22nd - 24th, virtual conference), pp. 399–406, 2020, https://doi.org/10.3384/ecp20176407

B. Stanmore, P. Gilot. Review – Calcination and carbonation of limestone during thermal cycling for CO_2 sequestration, *Fuel processing technology*, 86: 1707 – 1743, 2005

Lars-André Tokheim, Anette Mathisen, A., Lars E. Øi, Chameera Jayarathna, Nils H. Eldrup and Tor Gautestad. Combined calcination and CO_2 capture in cement clinker production by use of electrical energy, SINTEF proceedings, 4, pp 101-109, 2019

Ron Zevenhoven, Pia Kilpinen. Control of pollutants in flue gases and fuel gases, Helsinki University of Technology, 2001